Available online at www.sciencedirect.com
ScienceDirect
Geochimica et Cosmochimica Acta 73 (2009) 4400–4408
Geochimica et Cosmochimica Acta
www.elsevier.com/locate/gca

Experimental studies of oxygen isotope fractionation between rhodochrosite ($MnCO_3$) and water at low temperatures

Sang-Tae Kim [a,b,*], Jung Ok Kang [c], Seong-Taek Yun [c], James R. O'Neil [d], Alfonso Mucci [a]

[a] Department of Earth & Planetary Sciences, McGill University, Montreal, PQ, Canada H3A 2A7
[b] Department of Geology/ESSIC, University of Maryland, College Park, MD 20742, USA
[c] Department of Earth & Environmental Sciences and Environmental Geosphere Research Laboratory (EGRL), Korea University, Seoul 136-701, Republic of Korea
[d] Department of Geological Sciences, University of Michigan, Ann Arbor, MI 48109, USA

Received 10 September 2008; accepted in revised form 22 April 2009; available online 3 May 2009

Abstract

Rhodochrosite crystals were precipitated from Na–Mn–Cl–HCO_3 parent solutions following passive, forced and combined passive-to-forced CO_2 degassing methods. Forced and combined passive-to-forced CO_2 degassing produced rhodochrosite crystals with a small non-equilibrium oxygen isotope effect whereas passive CO_2 degassing protocols yielded rhodochrosite in apparent isotopic equilibrium with water. On the basis of the apparent equilibrium isotopic data, a new temperature-dependent relation is proposed for the oxygen isotope fractionation between rhodochrosite and water between 10 and 40 °C:

$$1000\ln\alpha_{\text{rhodochrosite–water}} = 17.84 \pm 0.18(10^3/T) - 30.24 \pm 0.62$$

or

$$1000\ln\alpha_{\text{rhodochrosite–water}} = 2.65 \pm 0.03(10^6/T^2) - 0.26 \pm 0.35$$

where $\alpha_{\text{rhodochrosite–water}}$ is the fractionation factor between rhodochrosite and water, and T is in kelvins. Over the temperature range investigated, rhodochrosite concentrates ^{18}O relative to both calcite and aragonite, a result that is consistent with the relative ionic radii of Ca^{2+} and Mn^{2+} and recent theoretical calculations.

1. INTRODUCTION

Manganese is a relatively abundant element on Earth and most commonly occurs in a variety of oxides, oxyhydroxides, and carbonates such as pyrolusite (MnO_2), manganite (MnO(OH)), rhodochrosite ($MnCO_3$), and kutnahorite ($CaMn(CO_3)_2$) in the Earth's crust. Rhodochrosite is isostructural with but less soluble and denser than calcite. It is typically found as an authigenic mineral in lacustrine and marine sediments (e.g., Morad and Al-Asam, 1997) or in hydrothermal ore deposits (e.g., So et al., 1993; Kuleshov and Bych, 2002). It was also reported in a Martian meteorite (e.g., Saxton et al., 2000).

Equilibrium oxygen isotope fractionations between various divalent metal carbonates and water have been measured experimentally by a number of researchers (e.g., O'Neil et al., 1969; Carothers et al., 1988; Kim and O'Neil, 1997; Jiménez-López et al., 2004) but few have focused on rhodochrosite. O'Neil et al. (1969) reported a rhodochrosite–water oxygen isotope fractionation of +7.26‰

* Corresponding author. Address: Department of Geology/ESSIC, University of Maryland, College Park, MD 20742, USA.
E-mail address: sangtae@umd.edu (S.-T. Kim).

0016-7037/$ - see front matter © 2009 Elsevier Ltd. All rights reserved.
doi:10.1016/j.gca.2009.04.018

(corrected for a fractionation factor of 1.0412 between $CO_{2(gas)}$ and H_2O) at 240 °C from a high temperature hydrothermal equilibration experiment. This result, combined with results of their calcite–water oxygen isotope fractionation study, indicated that rhodochrosite was depleted in ^{18}O by 0.4‰ relative to calcite at 240 °C. In contrast, their theoretical calculations predicted a positive (+0.7‰) oxygen isotope fractionation between rhodochrosite and calcite at the same temperature.

To resolve these discrepancies and better understand the oxygen isotope systematics of divalent metal carbonate–water systems, rhodochrosite was synthesized from aqueous solutions under well-controlled laboratory conditions at 10, 25 and 40 °C and the apparent equilibrium oxygen isotope fractionations between rhodochrosite and water were determined. Experimental protocols developed in previous studies of oxygen isotope fractionation in carbonate–water systems (e.g., Kim and O'Neil, 1997; Kim et al., 2007b) were employed to synthesize rhodochrosite.

2. EXPERIMENTAL METHOD

2.1. Synthesis of manganese carbonates

2.1.1. Forced CO_2 degassing methods

A 5 mmolal $NaHCO_3$ solution was prepared gravimetrically in deionized water (18 MΩ cm) and stored in a closed glass bottle immersed in a constant temperature bath at 10, 25 or 40 °C (±0.01 °C). The $NaHCO_3$ solution was aged for a minimum of 2 days to establish oxygen isotope equilibria among carbonic acid species in solution. The time required to reach oxygen isotopic equilibrium is a function of solution pH and temperature (Beck et al., 2005; Kim et al., 2006). Subsequently, reagent-grade $MnCl_2{\cdot}4H_2O$ was added to the isotopically- and thermally-equilibrated $NaHCO_3$ solution to a concentration of 5 mmolal Mn^{2+}. For the 40 °C experiments, purified CO_2 gas ($P = 1$ bar) was bubbled through the Na–Mn–Cl–HCO_3 solution for no more than 5 min in order to inhibit spontaneous nucleation and precipitation of rhodochrosite upon the addition of the $MnCl_2{\cdot}4H_2O$ salt. An aliquot of the Na–Mn–Cl–HCO_3 solution was taken for $\delta^{18}O$ analysis of the water and the pH was determined using a combination glass electrode calibrated at room temperature using two NIST-traceable buffer solutions (7.0 and 10.1 at 25 °C). Finally, 300 mL of the experimental solution were transferred into a specially designed glass vessel and the solution was thermostated for at least one hour in a constant temperature bath (±0.01 °C) before precipitation was initiated by stripping out the CO_2. Humidified N_2 gas was bubbled slowly through the experimental solution to remove CO_2 thus increasing the saturation state of the solution and promoting the nucleation and slow precipitation of rhodochrosite in the glass vessel. The N_2 gas was pre-saturated with water vapor by bubbling through a gas diffuser filled with water of the same oxygen isotope composition as the experimental solution in order to ensure that the oxygen isotope composition of the solution remained constant. After more than 10 mg of rhodochrosite precipitated (4 to 85 days), a 20 mL aliquot of the final experimental solution was taken for $\delta^{18}O$ analysis of the water, and the pH of the solution was measured. Rhodochrosite, precipitated on the walls and at the bottom of the glass vessel, was removed using a rubber policeman, filtered through a Gelman 0.45 μm Supor® membrane disk filter, and rinsed several times, first with large volumes (~2 L) of deionized water and then with methyl alcohol. The precipitates were dried on the filter paper for at least 10 h at 70 °C prior to storage for isotopic analysis. All precipitates were identified as pure rhodochrosite either by X-ray diffraction analysis, scanning electron microscopy (SEM), or optical microscopy. Fig. 1 shows typical XRD patterns of rhodochrosite crystals synthesized in this study at different temperatures.

A variant of the forced CO_2 degassing method was also employed at 40 °C. In this *passive-to-forced CO_2 degassing* method, CO_2 was degassed freely for several hours (or days) before water-saturated N_2 gas was bubbled though the experimental solution for the remainder of the precipitation experiment.

2.1.2. Passive CO_2 degassing methods

Na–Mn–Cl–HCO_3 solutions containing 3 or 5 mmolal Mn^{2+} were prepared as described in the previous Section 2.1.1. Two slightly different passive CO_2 degassing methods were used to precipitate rhodochrosite from the parent Na–Mn–Cl–HCO_3 solutions. In the first method, hereafter referred to as the *passive-1 CO_2 degassing* method, 1L of the experimental solution was kept in a thermostated, closed glass bottle throughout the course of precipitation and CO_2 was allowed to degas to the headspace (Kim et al., 2007b). In the second method, hereafter referred to as the *passive-2 CO_2 degassing* method, the experimental solution was allowed to degas freely to the atmosphere. In other words, the apparatus and protocols for the forced CO_2 degassing method were adopted without any modification except that N_2 gas was not bubbled through the solution. Collection of the initial and final experimental solutions for $\delta^{18}O$ analysis of the water and pH measurements of the solution were carried out as described in the previous section. Analysis of the oxygen isotope composition of the experimental solutions revealed that it remained invariant over the course of rhodochrosite precipitations (see Table 1). The rhodochrosite recovered at the end of these precipitation experiments was treated, examined, and stored as described in the previous section.

2.2. Oxygen isotope analysis

Rhodochrosite samples were reacted with fresh aliquots of phosphoric acid (i.e., $\rho = 1.92$ at 25 °C) at 77 °C for 15 min. An optimal reaction time of 15 min was chosen on the basis of time-series experiments carried out in this study. The CO_2 liberated from rhodochrosite by reaction with phosphoric acid was analyzed on a Finnigan MAT 251 or 253 stable isotope ratio mass spectrometer coupled to a Kiel I or IV device at the University of Michigan. Measured $\delta^{18}O$ values of the acid-liberated CO_2 ($\delta^{18}O_{CO_2(ACID)}$) at 77 °C from international reference standards NBS-18 and NBS-19 were fitted against their recommended $\delta^{18}O_{CO_2(ACID)}$ values at 77 °C. The recommended

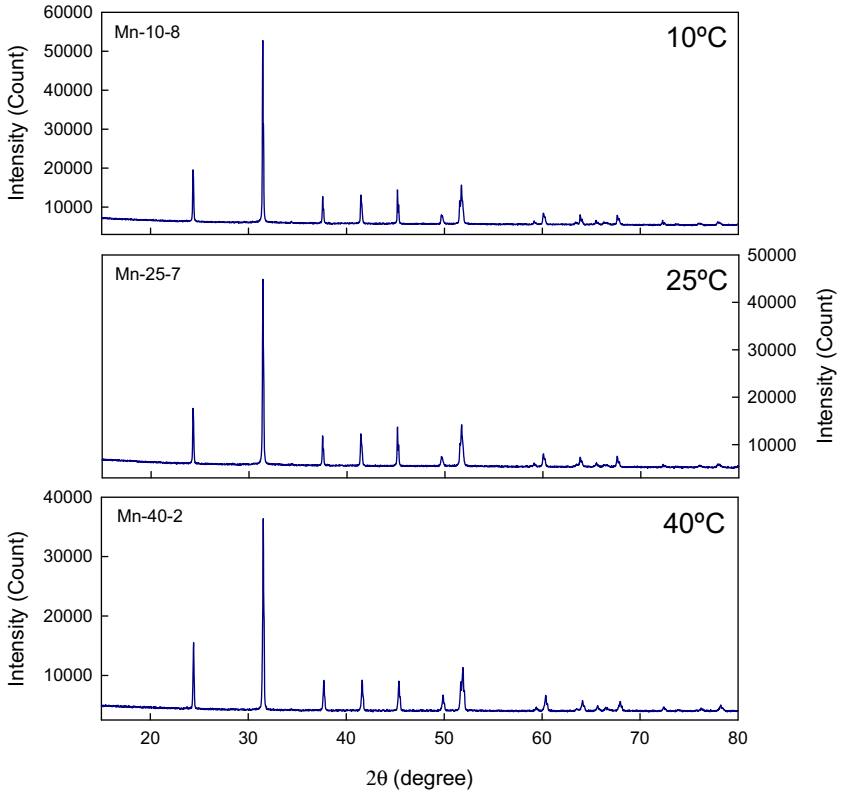

Fig. 1. Typical XRD patterns of rhodochrosite precipitates collected at three different temperatures for the calibration of the oxygen isotope fractionation between rhodochrosite and water.

$\delta^{18}O_{CO_2(ACID)}$ values of NBS-18 (+15.72‰) and NBS-19 (+37.39‰) at 77 °C were calculated on the basis of the acid fractionation factor of 1.00850 extrapolated to 77 °C from the temperature-relationship determined for calcite (Kim et al., 2007a) and the published $\delta^{18}O$ values for NBS-18 (+7.16‰) and NBS-19 (+28.65‰) relative to V-SMOW. Based on the calibration established above from the analyses of the international standards, $\delta^{18}O_{CO_2(ACID)}$ values of the rhodochrosite samples with respect to V-SMOW at 77 °C were estimated from the measured $\delta^{18}O_{CO_2(ACID)}$ values at 77 °C. The acid fractionation factor of 1.00796 at 77 °C for rhodochrosite (Sharma and Clayton, 1965; Böttcher, 1996) was then applied to the computed $\delta^{18}O_{CO_2(ACID)}$ values of the rhodochrosite samples. The reproducibility (1σ) of the $\delta^{18}O$ measurements, based upon replicate analyses of NBS-18 and NBS-19 standards under the same analytical conditions as of the rhodochrosite samples, was better than ±0.07‰.

Most of the water samples were analyzed at 25 °C using an automated CO_2–H_2O equilibration device coupled to a Finnigan MAT 252 stable isotope mass spectrometer at Korea University. A CO_2–H_2O fractionation factor of 1.0412 (O'Neil et al., 1975) was applied to obtain the oxygen isotope composition of the water itself, and the $\delta^{18}O$ values of water samples were normalized to the oxygen isotope compositions of two laboratory water standards calibrated against V-SMOW and V-SLAP. The overall precision (1σ) of the water $\delta^{18}O$ analyses, on the basis of replicate analyses of the laboratory water standards, was ±0.05‰. The other water samples, identified in Table 1, were analyzed using a Finnigan GasBench connected to a Finnigan DeltaPlus-XP stable isotope ratio mass spectrometer at the University of Ottawa (G.G. Hatch Stable Isotope Laboratory). In this case, samples and laboratory standards pre-pipetted into Exetainer® vials were equilibrated with a gas mixture of 2% CO_2 in helium at 25 °C or room temperature for a minimum of 18 h prior to the isotopic analysis of the CO_2. Analytical precision for this method was ±0.08‰ (1σ). The oxygen isotope fractionation factor between rhodochrosite and water ($\alpha_{rhodochrosite-water}$) is defined as:

$$\alpha_{rhodochrosite-water} = \frac{\delta^{18}O_{rhodochrosite} + 1000}{\delta^{18}O_{water} + 1000}$$

The permil fractionation ($1000\ln\alpha_{rhodochrosite-water}$) is used to present the experimental data in this study.

3. RESULTS AND DISCUSSION

3.1. Influence of precipitation rate on rhodochrosite–water fractionation

3.1.1. Synthesis method

Table 2 summarizes the results of individual precipitation experiments performed by each of the protocols described in this study and the averages of the rhodochrosite–water oxygen isotope fractionations ($1000\ln\alpha_{rhodochrosite-water}$) determined from the Mn–Na–Cl–HCO_3 parent solutions at

Table 1
Experimental conditions and oxygen isotope data for rhodochrosite precipitation experiments carried out at 10, 25, and 40 °C. Rhodochrosite was precipitated by forced or passive CO_2 degassing methods.

Sample	Temp. (°C)	HCO_3/Mn[a] (mmolal)	Method	Ini. S.I.	Initial pH	Final pH	$\delta^{18}O_{ini.\ water}$[b] (‰)	$\delta^{18}O_{rhodo.}$ (‰)	$\delta^{18}O_{water}$[c] (‰)	$\alpha_{(rhodo.–water)}$	1000ln $\alpha_{(rhodo.–water)}$
Mn-10-3	10.0	5/5[d]	Forced	2.98	7.86	7.46	−9.45	23.29	−9.44	1.03304	32.51
Mn-10-4	10.0	5/5	Forced	2.98	7.86	7.73	−9.45	23.16	−9.43	1.03290	32.37
Mn-10-5	10.0	5/5	Forced	2.98	7.78	7.32	−10.08	22.90	−9.70	1.03292	32.39
Mn-10-6	10.0	5/5	Forced	2.98	7.78	7.46	−10.08	23.06	−10.09	1.03349	32.94
Mn-10-7	10.0	5/5	Forced	2.98	7.78	7.60	−10.08	22.96	−10.02	1.03331	32.77
Mn-10-8	10.0	5/5	Forced	2.98	7.67	7.66	−9.84	23.15	−9.82	1.03330	32.75
Mn-10-9	10.0	5/5	Passive-2	2.98	7.67	7.17	−9.84	23.10	−9.73	1.03315	32.61
Mn-10-10	10.0	5/5	Passive-2	2.98	7.90	6.93	−9.93	23.03	−9.88	1.03324	32.70
Mn-10-11	10.0	5/5	Passive-2	2.98	7.90	6.94	−9.93	23.09	−9.90	1.03332	32.78
Mn-10-12	10.0	5/5	Passive-2	2.98	7.90	6.95	−9.93	23.02	−9.89	1.03324	32.70
Mn-10-13	10.0	5/5	Passive-1	2.98	7.78	6.98	−9.90	23.25	−9.87	1.03345	32.90
Mn-10-14	10.0	5/5	Passive-1	2.98	7.78	6.98	−9.89	23.07	−9.93	1.03333	32.79
Mn-10-15	10.0	5/5	Passive-1	2.98	7.79	6.90	−9.92	23.07	−9.91	1.03331	32.77
Mn-10-16	10.0	5/3	Passive-1	2.89	7.89	7.03	−9.94	23.04	−9.97	1.03334	32.80
Mn-10-17	10.0	5/3	Passive-1	2.89	7.88	7.07	−9.92	23.03	−9.96	1.03332	32.78
Mn-10-18	10.0	5/3	Passive-1	2.89	7.82	7.15	−9.90	23.02	−9.90	1.03325	32.71
Mn-25-1	25.0	5/5	Forced	3.09	7.83	7.42	−9.52	20.09	−9.52	1.02989	29.46
Mn-25-2	25.0	5/5	Forced	3.09	7.83	7.55	−9.52	20.01	−9.52	1.02981	29.38
Mn-25-3	25.0	5/5	Forced	3.09	7.83	7.54	−9.48	20.07	−9.54	1.02990	29.46
Mn-25-4	25.0	5/5	Forced	3.09	7.78	7.20	−9.52	20.21	−9.52	1.03002	29.57
Mn-25-5	25.0	5/5	Forced	3.09	7.78	7.33	−9.52	20.30	−9.49	1.03008	29.63
Mn-25-6	25.0	5/5	Forced	3.09	7.72	7.26	−10.07	19.36	−10.05	1.02971	29.28
Mn-25-7	25.0	5/5	Forced	3.09	7.72	7.43	−10.07	19.85	−10.00	1.03015	29.71
Mn-25-8	25.0	5/5	Passive-2	3.09	7.81	6.49	−9.96	20.28	−9.81	1.03039	29.94
Mn-25-9	25.0	5/5	Passive-2	3.09	7.81	6.79	−9.96	20.13	−9.88	1.03031	29.86
Mn-25-10	25.0	5/5	Passive-2	3.09	7.81	6.46	−9.96	20.14	−9.85	1.03029	29.84
Mn-25-11	25.0	5/5	Passive-1	3.09	7.77	6.74	−9.70[e]	20.00	−9.75[e]	1.02962	29.60
Mn-25-12	25.0	5/5	Passive-1	3.09	7.76	6.59	−9.76[e]	19.98	−9.77[e]	1.02963	29.60
Mn-25-13	25.0	5/5	Passive-1	3.09	7.68	6.58	−9.78[e]	20.02	−9.73[e]	1.02962	29.60
Mn-25-14	25.0	5/3	Passive-1	3.00	7.61	6.76	−9.78[e]	19.97	−9.76[e]	1.02960	29.58
Mn-25-15	25.0	5/3	Passive-1	3.00	7.61	6.82	−9.77[e]	19.97	−9.76[e]	1.02961	29.58
Mn-25-16	25.0	5/3	Passive-1	3.00	7.48	6.75	−9.76[e]	20.04	−9.72[e]	1.02964	29.61
Mn-40-1	40.0	5/5	Forced	3.54	6.69	7.11	−9.51	17.10	−9.43	1.02678	26.43
Mn-40-2	40.0	5/5	Forced	3.54	6.69	7.09	−9.51	17.05	−9.47	1.02677	26.42
Mn-40-3	40.0	5/5	Passive to forced	3.54	7.63	7.27	−10.11	16.59	−10.04	1.02690	26.54
Mn-40-4	40.0	5/5	Passive to forced	3.54	7.63	7.25	−10.11	16.49	−10.02	1.02678	26.43
Mn-40-5	40.0	5/5	Passive-2	3.54	7.63	7.18	−10.11	16.61	−10.05	1.02693	26.57
Mn-40-6	40.0	5/5	Passive to forced	3.54	7.83	7.45	−10.07	16.53	−10.06	1.02686	26.51
Mn-40-7	40.0	5/5	Passive to forced	3.54	7.83	7.22	−10.07	16.53	−10.02	1.02682	26.47
Mn-40-8	40.0	5/5	Passive to forced	3.54	7.83	7.27	−10.07	16.48	−10.07	1.02682	26.47
Mn-40-9	40.0	5/5	Passive-2	3.54	7.79	7.40	−10.04	16.52	−10.02	1.02681	26.46
Mn-40-10	40.0	5/5	Passive-2	3.54	7.79	7.32	−10.04	16.66	−10.03	1.02696	26.60
Mn-40-11	40.0	5/5	Passive-2	3.54	7.79	7.28	−10.04	16.67	−10.01	1.02695	26.59
Mn-40-12	40.0	5/5	Passive-1	3.54	7.52	6.53	−9.77[e]	17.10	−9.70[e]	1.02664	26.70
Mn-40-13	40.0	5/5	Passive-1	3.54	7.63	6.35	−9.77[e]	17.22	−9.76[e]	1.02682	26.88
Mn-40-14	40.0	5/5	Passive-1	3.54	7.68	6.29	−9.76[e]	17.29	−9.74[e]	1.02688	26.93
Mn-40-15	40.0	5/3	Passive-1	3.40	7.59	6.77	−9.76[e]	17.24	−9.71[e]	1.02680	26.85
Mn-40-16	40.0	5/3	Passive-1	3.40	7.73	6.58	−9.81[e]	17.03	−9.75[e]	1.02662	26.68
Mn-40-17	40.0	5/3	Passive-1	3.40	7.80	6.57	−9.54[e]	17.48	−9.50[e]	1.02681	26.87

Temp. = temperature; Ini. S.I. = initial saturation index; rhodo. = rhodochrosite.
[a] HCO_3/Mn denotes $NaHCO_3/MnCl_2{\cdot}4H_2O$.
[b] Oxygen isotope composition of the experimental solution at the beginning of the precipitation experiment.
[c] Oxygen isotope composition of the experimental solution at the end of the precipitation experiment.
[d] 5/5 denotes 5 mmolal $NaHCO_3$ + 5 mmolal $MnCl_2{\cdot}4H_2O$.
[e] Denotes a value obtained from the Univerity of Ottawa.

10, 25, and 40 °C. Considering the analytical error ($1\sigma_{analytical} = \pm 0.13$ or ± 0.15‰, see Table 2) associated with the oxygen isotope analyses of rhodochrosite and water, slightly smaller averages (maximum differences of 0.20,

Table 2
The type and number of precipitation experiments, average values of $1000\ln\alpha_{rhodochrosite-water}$, their corresponding standard deviations, and analytical errors at 10, 25, and 40 °C.

	Temperature/Synthesis method	n	$1000\ln\alpha_{rhodochrosite-water}$	σ	s_e	$\alpha_{analytical}$
10 °C						
	Forced CO_2 degassing	6	32.62	0.21	0.09	0.13
	Passive-1 CO_2 degassing	3	32.82	0.06	0.03	0.13
	Passive-2 CO_2 degassing	4	32.70	0.06	0.03	0.13
25 °C						
	Forced CO_2 degassing	7	29.50	0.14	0.05	0.13
	Passive-1 CO_2 degassing	3	29.60	0.00	0.00	0.15
	Passive-2 CO_2 degassing	3	29.88	0.04	0.02	0.13
40 °C						
	Forced CO_2 degassing	2	26.43	0.00	0.00	0.13
	Passive-to-forced CO_2 degassing	5	26.48	0.04	0.02	0.13
	Passive-1 CO_2 degassing	3	26.84	0.10	0.06	0.15
	Passive-2 CO_2 degassing	4	26.56	0.06	0.03	0.13

n = number of experiment; σ = standard deviation; $\sigma_{analytical}$ = maximum analytical error; s_e = standard error.

0.38 and 0.41‰ at 10, 25, and 40 °C, respectively) of the $1000\ln\alpha_{rhodochrosite-water}$ were determined from the rhodochrosite prepared by the forced (forced and passive-to-forced) CO_2 degassing methods. We ascribe the discrepancy to a non-equilibrium isotope or kinetic effect resulting from the faster precipitation of rhodochrosite in the forced CO_2 degassing experiments relative to the passive-1 and passive-2 CO_2 degassing experiments.

Kim and O'Neil (1997) and Kim et al. (2007b) demonstrated that calcite and aragonite were precipitated in isotopic equilibrium with the parent solutions under their experimental conditions (e.g., *slow* bubbling rate, 5 mmolal Ca^{2+} and HCO_3^- initial concentrations) by the forced CO_2 degassing method. Rhodochrosite is, however, approximately 100 times less soluble than calcite in water (Morse and Mackenzie, 1990) and, under similar experimental conditions (5 mmolal Mn^{2+} and HCO_3^- initial concentrations), precipitation rates in forced CO_2 degassing experiments should be much larger. Accordingly, the oxygen isotope fractionation between rhodochrosite and water is expected to be more susceptible to non-equilibrium isotope or kinetic effects when the mineral is precipitated by this method. Similarly, Kim et al. (2006) reported non-equilibrium isotope effects when aragonite and witherite were precipitated rapidly at 25 °C and proposed that the effects were related to the fast precipitation of the carbonate minerals.

It is noteworthy that the smallest non-equilibrium isotope or kinetic effect (0.20‰) was observed at the lowest investigated temperature (10 °C) where the slowest precipitation rate is expected since rhodochrosite displays retrograde solubility (Bethke, 1998) and, hence, the initial saturation index ($\log[\{Mn^{2+}\} \times \{CO_3^{2-}\}/K°_{sp\ (rhodochrosite)}]$ where $\{Mn^{2+}\}$ and $\{CO_3^{2-}\}$ are the activities of the Mn^{2+} and CO_3^{2-} ions, respectively) of the parent solution will be lower at lower temperatures. The initial saturation index of the parent Na–Mn–Cl–HCO_3 solution for each synthesis experiment, with respect to rhodochrosite, was calculated using the Geochemist Work-bench® (B-dot equation, an extended form of the Debye–Hűckel equation described by Helgeson (1969)) from the gravimetric recipe (Mn^{2+}, carbonate alkalinity, and total dissolved inorganic carbon concentrations) and is reported in Table 1. Because the rhodochrosite crystals prepared by the forced CO_2 degassing methods formed out of oxygen isotope equilibrium with the ambient water, only the data collected for rhodochrosite prepared by the passive CO_2 degassing methods were used to calculate our best estimate of the equilibrium oxygen isotope fractionation between rhodochrosite and water.

3.1.2. Initial Mn^{2+} concentration

Under the experimental conditions investigated by Kim et al. (2006, 2007b), it can be inferred from their oxygen isotope data that the initial Ca^{2+} concentrations and alkalinities of the experimental solutions did not influence the "equilibrium" oxygen isotope fractionation between aragonite and water. Isotopic equilibrium between a precipitating carbonate mineral and its parent solution can be achieved, regardless of the chemical composition of the solution, when (1) the carbonate mineral precipitates slowly enough for the adsorbed CO_3^{2-} and/or the newly formed carbonate surface layer to equilibrate with the surrounding water and (2) dissolved ions, such as Ca^{2+} and Mg^{2+}, in the precipitating solution do not modify the physical and chemical properties of water molecules in the solution and do not significantly alter the precipitation mechanism.

To confirm that oxygen isotope equilibrium was established in the synthetic rhodochrosite prepared by the two passive CO_2 degassing methods (passive-1 and passive-2), rhodochrosite was precipitated using the same method but from Na–Mn–Cl–HCO_3 solutions of lower initial Mn^{2+} concentrations (3 instead of 5 mmolal). By lowering the initial Mn^{2+} concentration of the parent solution and, hence, its initial saturation index, the precipitation rate will decrease and minimize kinetic effects that might arise during mineral growth. Table 3 shows the averages, standard deviations, and analytical errors of the permil rhodochrosite–water oxygen isotope fractionation ($1000\ln\alpha_{rhodochrosite-water}$) for samples precipitated from Na–Mn–Cl–HCO_3 solutions of different initial Mn^{2+} concentrations at 10, 25, and 40 °C. The 1σ values, reported in Table 3, are standard deviations of the experimentally-determined permil fractionations

Table 3
The conditions and number of precipitation experiments, average values of $1000\ln\alpha_{rhodochrosite-water}$, their corresponding standard deviations, and analytical errors at 10, 25, and 40 °C.

Temperature/Initial concentrations	n	Method	$1000\ln\alpha_{rhodochrosite-water}$	σ	$\sigma_{analytical}$
10 °C					
5 mmolal $NaHCO_3$ + 3 mmolal $MnCl_2{\cdot}4H_2O$	3	Passive-1	32.76	0.04	0.13
5 mmolal $NaHCO_3$ + 5 mmolal $MnCl_2{\cdot}4H_2O$	3	Passive-1	32.82	0.06	0.13
5 mmolal $NaHCO_3$ + 5 mmolal $MnCl_2{\cdot}4H_2O$	7	Passive-1&2	32.75	0.08	0.13
25 °C					
5 mmolal $NaHCO_3$ + 3 mmolal $MnCl_2{\cdot}4H_2O$	3	Passive-1	29.59	0.01	0.15
5 mmolal $NaHCO_3$ + 5 mmolal $MnCl_2{\cdot}4H_2O$	3	Passive-1	29.60	0.00	0.15
5 mmolal $NaHCO_3$ + 5 mmolal $MnCl_2{\cdot}4H_2O$	6	Passive-1&2	29.74	0.14	0.15
40 °C					
5 mmolal $NaHCO_3$ + 3 mmolal $MnCl_2{\cdot}4H_2O$	3	Passive-1	26.80	0.09	0.15
5 mmolal $NaHCO_3$ + 5 mmolal $MnCl_2{\cdot}4H_2O$	3	Passive-1	26.84	0.10	0.15
5 mmolal $NaHCO_3$ + 5 mmolal $MnCl_2{\cdot}4H_2O$	7	Passive-1&2	26.68	0.16	0.15

n = number of experiment; σ = standard deviation; $\sigma_{analytical}$ = maximum analytical error.

($1000\ln\alpha_{rhodochrosite-water}$) under a given set of experimental conditions. Analytical errors (Section 2.2) associated with the oxygen isotope composition measurements of rhodochrosite and water are not reflected in these values. Within the analytical error ($1\sigma_{analytical} = \pm 0.13$ or $\pm 0.15‰$) (Tables 2 and 3) and the range of concentrations and temperatures investigated, the initial Mn^{2+}concentration of the parent solutions does not affect the oxygen isotope fractionation between rhodochrosite and water (Fig. 2). These results are consistent with the assumption, in accordance with the hypothesis of Kim et al. (2006, 2007b), that "equilibrium" carbonate–water fractionation can be achieved irrespective of the initial concentration of the parent solutions. Accordingly, the $1000\ln\alpha_{rhodochrosite-water}$ values obtained by the two passive CO_2 degassing methods, regardless of the initial cation concentrations investigated, were considered as "apparent equilibrium" permil oxygen isotope fractionations between rhodochrosite and water.

Kim and O'Neil (1997) observed positive and reproducible *non-equilibrium* isotope effects for calcite, witherite, and otavite crystals synthesized from Na–X–Cl–HCO_3 (X = Ca^{2+}, Cd^{2+}, or Ba^{2+}) solutions at high initial cation concentrations and carbonate alkalinities. The observed *non-equilibrium* isotope effects could have been kinetic in origin and possibly due to the relatively high precipitation rates of the carbonates from highly supersaturated solutions. Alternatively, the reproducible experimental fractionations, as a function of both solution composition and temperature, could be interpreted as reflecting *isotopic equilibrium* with the solution since water bound to dissolved electrolytes in concentrated solutions can have distinctly different isotopic properties from those of the pure or bulk water (O'Neil and Truesdell, 1991; Horita et al., 1993a; Horita et al., 1993b).

3.2. Temperature dependence of rhodochrosite–water fractionation

Twenty nine samples of rhodochrosite were precipitated between 10 and 40 °C by the two passive-CO_2 degassing methods and their oxygen isotope compositions were measured. The temperature dependence of the rhodochrosite–water oxygen isotope fractionation between 10 and 40 °C is shown in Fig. 3 and the new calibration is given by the following expression:

$$1000\ln\alpha_{rhodochrosite-water} = 17.84 \pm 0.18(10^3/T) - 30.24 \pm 0.62 \quad (1)$$

or

$$1000\ln\alpha_{rhodochrosite-water} = 2.65 \pm 0.03(10^6/T^2) - 0.26 \pm 0.35 \quad (2)$$

The slope of the inverse-temperature ($1/T$, Eq. (1)) rhodochrosite–water fractionation relation (17.84 ± 0.18) is statistically indistinguishable from that of the calcite–water (18.03; Kim and O'Neil, 1997) and aragonite–water (17.88 ± 0.13; Kim et al., 2007) calibrations. It should be noted that reported uncertainties for the slope and intercept in Eq. (1) are based on the 29 experimentally-determined values of $1000\ln\alpha_{rhodochrosite-water}$ and analytical errors reported in Section 2.2 are not taken into account in their derivation.

3.3. Comparison with theoretical calculations

Theoretical and experimental fractionation curves for the rhodochrosite–water, aragonite–water, and calcite–water systems are shown in Fig. 4. A most important feature of the fractionation curves shown in Fig. 4 is the order of relative equilibrium ^{18}O enrichment among the Ca and Mn carbonates: rhodochrosite > aragonite > calcite. The positive experimental rhodochrosite–calcite fractionations at low temperatures (e.g., +1.5‰ at 25 °C) are consistent with the fractionations calculated by O'Neil et al. (1969) at high temperatures (+0.7‰ at 240 °C). Results of a more recent theoretical study by Chacko and Deines (2008) also yield positive rhodochrosite–calcite fractionations (+2.5 and +0.9‰ at 25 and 240 °C, respectively). The theoretical and experimental oxygen isotope fractionation calibration curves for the rhodochrosite–water, aragonite–water, and calcite–water systems are in relatively good agreement given the standard errors (±0.62‰ in the case of the rhodochrosite–water system) of the regression analysis in the experimental calibrations. Based upon the results of this oxygen

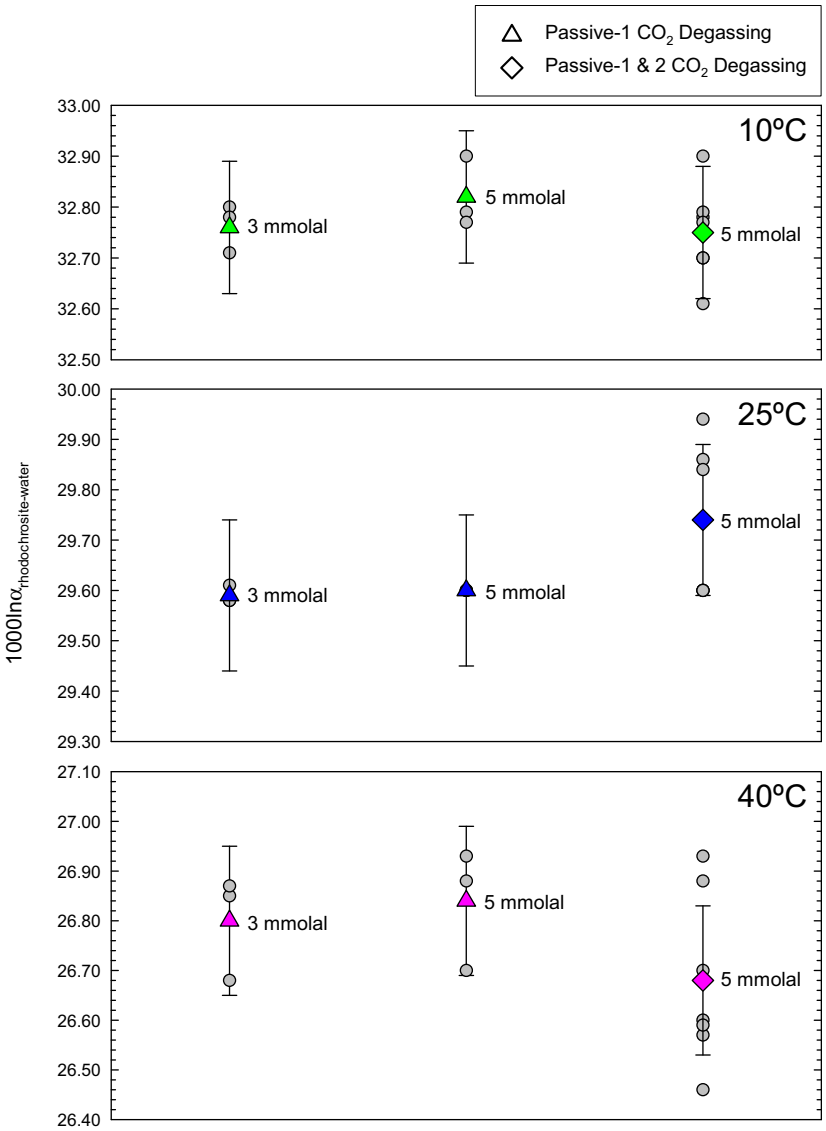

Fig. 2. Effect of initial Mn^{2+} concentration on $1000\ln\alpha_{rhodochrosite-water}$ at 10, 25, and 40 °C. Circles represent individual permil fractionations ($1000\ln\alpha_{rhodochrosite-water}$) determined in this study by the two passive CO_2 degassing methods. Each triangle or diamond represents the average of the permil fractionations. The vertical bars associated with the averages correspond to the analytical error (±0.13‰ or ±0.15‰). Within these errors, the initial Mn^{2+} concentration (or precipitation rate) had no significant influence on the isotopic composition of the precipitate under the conditions investigated in this study.

isotope calibration study, the cation radius appears to be a critical factor in determining the equilibrium isotope properties of carbonate minerals. Given the dearth of experimental results on this system, further laboratory studies are required to unambiguously determine which parameters (e.g., cation radius or reduced mass) governs the equilibrium oxygen isotope fractionation in carbonate minerals.

4. CONCLUSIONS

Forced CO_2 degassing precipitation methods yielded rhodochrosite that incorporated a small non-equilibrium oxygen isotope or kinetic effect. Conversely, two passive CO_2 degassing methods, applied under various experimental conditions, produced rhodochrosite in apparent oxygen isotope equilibrium with water in the parent solutions. These data were chosen to derive the following equations that describe low-temperature oxygen isotope fractionation between rhodochrosite and water:

$$1000\ln\alpha_{rhodochrosite-water} = 17.84 \pm 0.18(10^3/T) - 30.24 \pm 0.62$$

$$\text{or } 1000\ln\alpha_{rhodochrosite-water} = 2.65 \pm 0.03(10^6/T^2) - 0.26 \pm 0.35$$

A combination of this new experimental calibration with published calibrations for aragonite and calcite establishes that, at equilibrium, rhodochrosite concentrates ^{18}O relative to aragonite which, in turn, concentrates ^{18}O relative to calcite. This experimental observation is consistent with results of recent and previous theoretical estimates of oxygen isotope fractionation factors in carbonate systems and

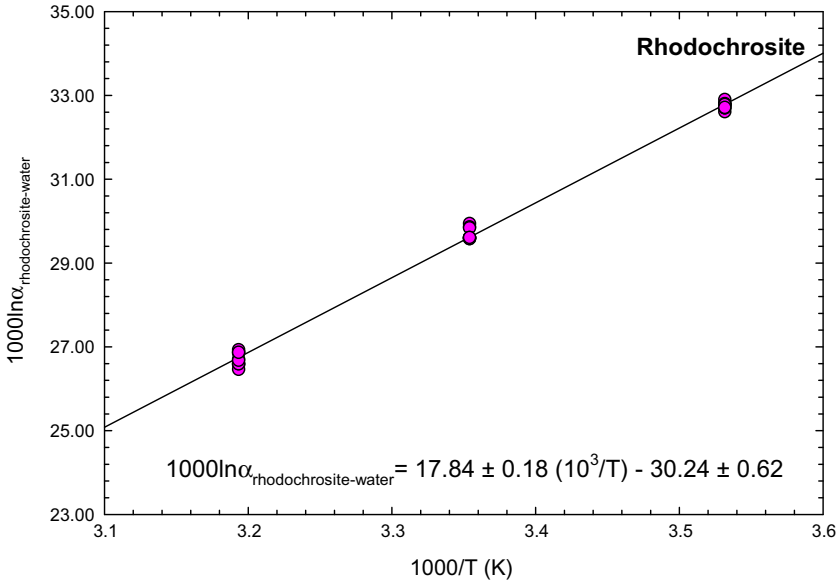

Fig. 3. Relation between $1000\ln\alpha_{\text{rhodochrosite–water}}$ and temperature. The temperature dependence of the oxygen isotope fractionation between rhodochrosite and water (Eq. (1)) is calibrated on the basis of the equilibrium isotope composition of rhodochrosites synthesized from Na–Mn–Cl–HCO_3 solutions by the passive CO_2 degassing methods between 10 and 40 °C.

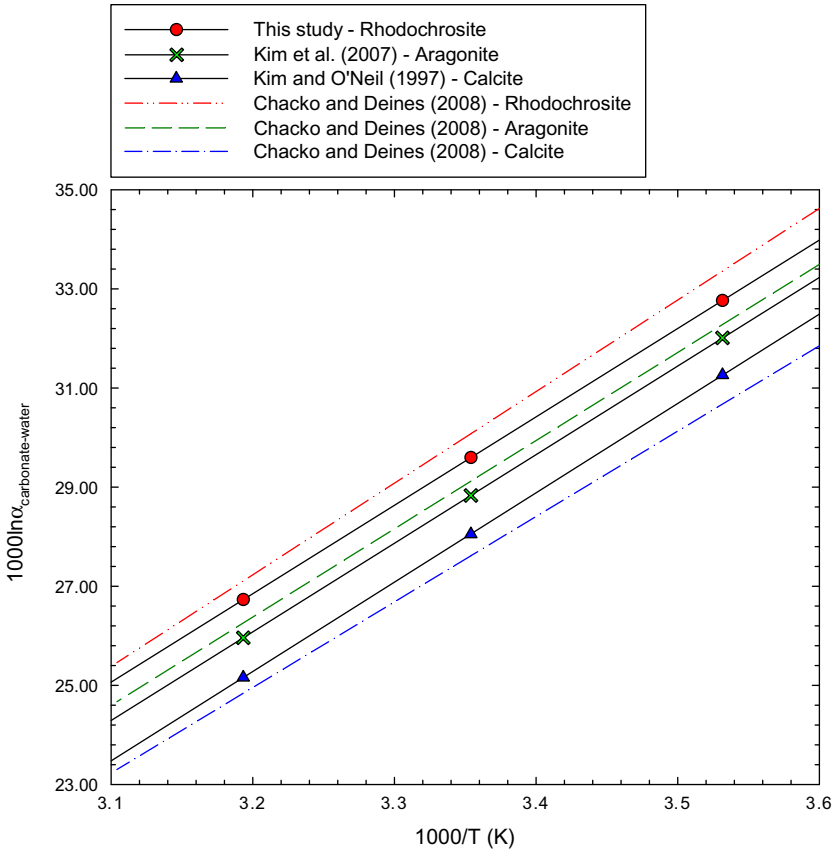

Fig. 4. Comparison of experimental (solid lines with symbols: this study; Kim et al., 2007; Kim and O'Neil, 1997) and theoretical (dashed lines without symbols: Chacko and Deines, 2008) oxygen isotope fractionation curves for the rhodochrosite–water, aragonite–water, and calcite–water systems at low temperatures.

furthers our understanding of the oxygen isotope geochemistry of divalent metal carbonates.

ACKNOWLEDGMENTS

This research was initiated while one of the authors (S.-T. Kim) was visiting the stable isotope laboratory of the Center for Mineral Resources Research (CMR) at Korea University. The authors acknowledge CMR for providing access to its stable isotope laboratory facilities. This research was funded by a grant from the Environmental Geosphere Research Laboratory (EGRL) of Korea University to S.-T. Yun and a NSERC Discovery grant to A.M. The authors would like to thank Lora Wingate and C.-S. Kim for their assistance in the laboratory. Finally, the authors wish to acknowledge Drs. Gilg, Romanek, Chacko and one anonymous reviewer for their constructive comments/recommendations on the original version of this manuscript.

REFERENCES

Beck W. C., Grossman E. L. and Morse J. W. (2005) Experimental studies of oxygen isotope fractionation in the carbonic acid system at 15°, 25°, and 40 °C. *Geochim. Cosmochim. Acta* **69**, 3493–3503.

Bethke C. M. (1998) *The Geochemist's Workbench, Version 3.0: A Users Guide to Rxn, Act2, Tact, React, and Gtplot*. Hydrogeology Program, University of Illinois, Urbana.

Böttcher M. E. (1996) $^{18}O/^{16}O$ and $^{13}C/^{12}C$ fractionation during the reaction of carbonates with phosphoric acid: effects of cationic substitution and reaction temperature. *Isotopes Environ. Health Stud.* **32**, 299–305.

Carothers W. W., Adami L. H. and Rosenbauer R. J. (1988) Experimental oxygen isotope fractionation between siderite–water and phosphoric acid liberated CO_2–siderite. *Geochim. Cosmochim. Acta* **52**, 2445–2450.

Chacko T. and Deines P. (2008) Theoretical calculation of oxygen isotope fractionation factors in carbonate systems. *Geochim. Cosmochim. Acta* **72**, 3642–3660.

Helgeson H. C. (1969) Thermodynamics of hydrothermal systems at elevated temperatures and pressures. *Am. J. Sci.* **267**, 729–804.

Horita J., Cole D. R. and Wesolowski D. J. (1993a) The activity-composition relationship of oxygen and hydrogen isotopes in aqueous salt solutions: II. Vapor–liquid water equilibration of mixed salt solutions from 50 to 100 °C and geochemical implications. *Geochim. Cosmochim. Acta* **57**, 4703–4711.

Horita J., Wesolowski D. J. and Cole D. R. (1993b) The activity-composition relationship of oxygen and hydrogen isotopes in aqueous salt solutions: I. Vapor–liquid water equilibration of single salt solutions from 50 to 100 °C. *Geochim. Cosmochim. Acta* **57**, 2797–2817.

Jiménez-López C., Romanek C. S., Huertas F. J., Ohmoto H. and Caballero E. (2004) Oxygen isotope fractionation in synthetic magnesian calcite. *Geochim. Cosmochim. Acta* **68**, 3367–3377.

Kim S.-T., Hillaire-Marcel C. and Mucci A. (2006) Mechanisms of equilibrium and kinetic oxygen isotope effects in synthetic aragonite at 25 °C. *Geochim. Cosmochim. Acta* **70**, 5790–5801.

Kim S.-T., Mucci A. and Taylor B. E. (2007a) Phosphoric acid fractionation factors for calcite and aragonite between 25 and 75 °C: revisited. *Chem. Geol.* **246**, 135–146.

Kim S.-T. and O'Neil J. R. (1997) Equilibrium and nonequilibrium oxygen isotope effects in synthetic carbonates. *Geochim. Cosmochim. Acta* **61**, 3461–3475.

Kim S.-T., O'Neil J. R., Hillaire-Marcel C. and Mucci A. (2007b) Oxygen isotope fractionation between synthetic aragonite and water: influence of temperature and Mg^{2+} concentration. *Geochim. Cosmochim. Acta* **71**, 4704–4715.

Kuleshov V. N. and Bych A. F. (2002) Isotopic composition ($\delta^{13}C$, $\delta^{18}O$) and origin of manganese carbonate ore of the Usa deposit (Kuznetskii Alatau). *Lithol. Miner. Resour.* **37**, 330–343.

Morad S. and Al-Asam I. S. (1997) Conditions of rhodochrosite-nodule formation in Neogene–Pleistocene deep-sea sediments: evidence from O, C, and Sr isotopes. *Sediment. Geol.* **114**, 295–304.

Morse J. W. and Mackenzie F. T. (1990) *Geochemistry of Sedimentary Carbonates*. Elsevier, Amsterdam.

O'Neil J. R., Adami L. H. and Epstein S. (1975) Revised value for the O^{18} fractionation between CO_2 and H_2O at 25 °C. *J. Res. US Geol. Surv.* **3**, 623–624.

O'Neil J. R., Clayton R. N. and Mayeda T. K. (1969) Oxygen isotope fractionation in divalent metal carbonates. *J. Chem. Phys.* **51**, 5547–5558.

O'Neil J. R. and Truesdell A. H. (1991) Oxygen isotope fractionation studies of solute–water interactions. In *Stable Isotope Geochemistry: A Tribute to Samuel Epstein* (eds. H. P. Taylor Jr., J. R. O'Neil and I. R. Kaplan). The Geochemical Society, San Antonio., pp. 17–25.

Saxton J. M., Lyon I. C., Chatzitheodoridis E. and Turner G. (2000) Oxygen isotopic composition of carbonate in the Nakhla meteorite: implication for the hydrosphere and atmosphere of Mars. *Geochim. Cosmochim. Acta* **64**, 1299–1309.

Sharma T. and Clayton R. N. (1965) Measurement of O^{18}/O^{16} ratios of total oxygen of carbonates. *Geochim. Cosmochim. Acta* **29**, 1347–1353.

So C. S., Yun S. T. and Koh Y. K. (1993) Mineralogic, fluid inclusion, and stable isotope evidence for the genesis of carbonate-hosted Pb–Zn (–Ag) orebodies of the Taebaek deposit, Republic of Korea. *Econ. Geol.* **88**, 855–872.

Associate editor: Thomas Chacko